

THERMALLY STIMULATED LUMINESCENCE EXCITATION SPECTROSCOPY  
AS A TECHNIQUE TO MEASURE THE PHOTOIONIZATION ENERGY OF  
 $\text{Sr}(\text{SCN})_2:\text{Eu}^{2+}$

by

BO WEN

(Under the direction of Uwe Happek)

ABSTRACT

$\text{Sr}(\text{SCN})_2:\text{Eu}^{2+}$  (Strontium Thiocyanates doped with Europium 2+) shows strong luminescence quenching at relatively low temperatures. It has been suggested that this quenching is due to the thermal promotion of the excited electrons into the conduction band, followed by nonradiative relaxation back to the ground state. In this thesis we report on experiments to confirm the quenching mechanism in  $\text{Sr}(\text{SCN})_2:\text{Eu}^{2+}$ . Because the sample is highly hygroscopic and has to be kept sealed in a quartz vial under an argon atmosphere, the experimental determination of the ionization onset is challenging. We are using thermally stimulated luminescence (TSL) as a non-contact technique to probe the onset between the impurity ground state relative to the host conduction band. We confirm that the quenching in  $\text{Sr}(\text{SCN})_2:\text{Eu}^{2+}$  is due to photo-ionization.

INDEX WORDS: Thermally Stimulated Luminescence, Photoionization ,  
Hygroscopic

THERMALLY STIMULATED LUMINESCENCE EXCITATION SPECTROSCOPY  
AS A TECHNIQUE TO MEASURE THE PHOTOIONIZATION ENERGY OF  
 $\text{Sr}(\text{SCN})_2:\text{Eu}^{2+}$

by

BO WEN

B.S., Zhongshan University, P.R. China, 1999

A Thesis Submitted to the Graduate Faculty  
of The University of Georgia in Partial Fulfillment  
of the  
Requirements for the Degree

MASTER OF SCIENCE

ATHENS, GEORGIA

2004

© 2004

Bo Wen

All Rights Reserved

THERMALLY STIMULATED LUMINESCENCE EXCITATION SPECTROSCOPY  
AS A TECHNIQUE TO MEASURE THE PHOTOIONIZATION ENERGY OF  
 $\text{Sr}(\text{SCN})_2:\text{Eu}^{2+}$

by

BO WEN

Approved:

Major Professor: Uwe Happek

Committee: W. Gary Love  
William M. Dennis

Electronic Version Approved:

Maureen Grasso  
Dean of the Graduate School  
The University of Georgia  
Dec 2004

## DEDICATION

To Dad and Mom.....

## ACKNOWLEDGMENTS

Thanks to Dr. Happek who gave me all the support and inspiration to finish this thesis and Dr. C. Wickleder who prepared the sample for the experiment. Thanks also to Dr. Bill Dennis and Dr. W. Gary Love who served as my committee members and corrected my thesis. Thanks to Dr. Jay Fleniken who helped me through a lot of difficulties and taught me a lot of techniques needed for the experiment. Thanks also to all the other group members, Paul Schmidt, Long Pham and especially Steve Cox for their support during the difficult times.

This work was supported in part by a grant from the U.S. Department of Energy, grant # DE-FC26.04NT41956, and by General Electric.

## TABLE OF CONTENTS

	Page
DEDICATION . . . . .	iv
ACKNOWLEDGMENTS . . . . .	v
LIST OF FIGURES . . . . .	viii
CHAPTER	
1 INTRODUCTION . . . . .	1
2 ELECTRON TRANSFER PROCESSES IN DOPED CRYSTALS . . . . .	3
2.1 BAND STRUCTURE OF SOLIDS . . . . .	3
2.2 LOCALIZED ENERGY LEVELS . . . . .	4
2.3 PHOTOIONIZATION AND CHARGE TRANSFER . . . . .	6
3 THEORY OF THERMOLUMINESCENCE . . . . .	11
3.1 LUMINESCENCE . . . . .	11
3.2 PHOSPHORESCENCE . . . . .	11
3.3 THERMOLUMINESCENCE . . . . .	14
3.4 GLOW CURVE ANALYSIS . . . . .	14
4 THERMOLUMINESCENCE EXPERIMENT . . . . .	20
4.1 THERMALLY STIMULATED LUMINESCENCE EXCITATION SPECTROSCOPY (TSLES) . . . . .	20
4.2 EXPERIMENTAL EQUIPMENT AND SETUP . . . . .	21
4.3 TYPICAL CRYOSTAT DESIGN . . . . .	21

	vii
4.4 EXPERIMENT RESULTS . . . . .	37
5 CONCLUSIONS . . . . .	41
5.1 REFERENCES . . . . .	42

## LIST OF FIGURES

2.1	Band Structure of Insulater . . . . .	5
2.2	Electron transitions in insulators . . . . .	8
2.3	Electron transitions in insulators . . . . .	9
2.4	Electron transitions in insulators . . . . .	10
3.1	Fluorescence and phosphorescence . . . . .	13
3.2	Typical Thermally Stimulated Luminescence glow curves Excited at different wavelength . . . . .	15
3.3	Process during irradiation . . . . .	16
3.4	The relation between the untrapping probability, luminescent inten- sity, and trapped charge population. . . . .	18
4.1	The Principle of using TSL to locate the ground state of impurity . .	22
4.2	A Thermally Stimulated Luminescence Excitation Spectroscopy TSLES	23
4.3	Design of the sample chamber . . . . .	24
4.4	The sample cryostat used in the experiment . . . . .	26
4.5	Experimental Setup . . . . .	27
4.6	Temperature dependance of emission . . . . .	30
4.7	Excitation and emission spectrum from Dr. Wickleder . . . . .	31
4.8	The emission and excitation spectrum obtained in the lab . . . . .	32
4.9	Crystal structure of $\text{Ba}(\text{SCN})_2:\text{Eu}^{2+}$ . . . . .	33
4.10	Energy level graph . . . . .	35
4.11	The temperature dependance of $\text{Sr}(\text{SCN})_2:\text{Eu}^{2+}$ . . . . .	36

4.12	The glow curves of $\text{Sr}(\text{SCN})_2:\text{Eu}^{2+}$ . . . . .	38
4.13	The TSLES of $\text{Sr}(\text{SCN})_2:\text{Eu}^{2+}$ . . . . .	39

## CHAPTER 1

### INTRODUCTION

In the study of phosphors, radiative and nonradiative relaxation are two important mechanisms which affect the luminescence of the material of interest. The excited electrons of the impurities can be thermally promoted into the conduction band followed by nonradiative relaxation, thus no luminescence can be observed. Therefore the placement of impurity energy levels relative to the host conduction or valence band is of great importance.

For an ideal crystal there are no energy levels between the conduction band and valence band. However, when impurities are present, some of the impurity energy levels may be found in the region of the host energy gap. The charge transfer processes between these discrete energy levels and the host bands are often overlooked at the expense of intra-ion transitions [1], but for transitions under illumination in the UV or VUV region, these transitions become very important [2] .

If by any means the electrons of the impurities get excited into the conduction band, a fraction of these electrons may be captured by so-called traps. These traps will lead to thermal luminescence, and phosphorescence in general. If a non-radiative relaxation channel exists between the conduction band and the impurity ground state, promotion of impurity electrons will lead to quenching, in extreme cases no luminescence will be observed at all.

This thesis will present a technique called Thermally Stimulated Luminescence (TSL) to study the charge transfer processes in insulators. This technique is used

for a variety of applications, including dosimetry, archeology, dating, and the study of shallow traps [7].

Here we are using thermoluminescence as a spectroscopy tool to measure the ionization energy of dopants, by applying TSL as a form of excitation spectroscopy. Compared to other techniques such as photoconductivity or photoelectron spectroscopy, this technique has a number of advantages, including high sensitivity, non-contact probing, site and impurity specific signals, and applicability to single crystalline, polycrystalline, and amorphous samples.

In this thesis, we attempt to measure the ionization energy of  $\text{Eu}^{2+}$  in  $\text{Sr}(\text{SCN})_2$ , a system that is challenging due to the fact that this sample is very sensitive to moisture in the air and thus has to be sealed inside a quartz vial under argon atmosphere. Moreover, in this sample the luminescence quenches at very low temperatures, this makes thermoluminescence studies which, by definition, rely on the observation of luminescence at elevated temperatures, very difficult.

## CHAPTER 2

### ELECTRON TRANSFER PROCESSES IN DOPED CRYSTALS

#### 2.1 BAND STRUCTURE OF SOLIDS

An ideal crystal is constructed by the infinite repetition of identical structural units in space[4]. The structure of all crystals can be described in terms of a lattice. There are many different kinds of crystal lattices and they are classified, in general, according to their symmetries, which specify invariant properties for translational and rotational operations[5].

When atoms are brought together to form a solid, they approach each other and the wave functions of these atoms start to overlap. According to Pauli, electrons of the same orbital must occupy different states, forming a band of states instead of a discrete level as in the isolated atom [3]. In insulators, the energy bands are either completely filled or empty at zero temperature, and the energetically highest filled band is called the valence band, and the energetically lowest empty band is called the conduction band. A completely filled valence band cannot support a current, and an electron has to be promoted into the conduction band, where it will drift, directed under the influence of an electric field or randomly due to thermal energy.

The zone between the bottom of conduction band and top of the valence band is called the band gap, and no localized discrete energy levels can exist between the energy gap in a ideal crystal. An electron can be excited from the valence band to the conduction band via absorption of energy such as light, particle impact, or heat. The excited electron leaves a hole in the valence band, and both the electron and

hole are mobile until they recombine. The schematic diagram of these excitations is shown in Figure 2.1. The band gap of a material is strongly related to the optical properties and to the electric conductivity of crystals[5].

If the crystal contains some kinds of impurities these might have discrete energy levels that have a binding energy that lies in the region between the top of the valence and bottom of the conduction band.

## 2.2 LOCALIZED ENERGY LEVELS

In the previous section we saw that several forbidden zones (in terms of energy) for electrons exist in a solid, due to the translational symmetry of the crystal structure. Furthermore, the forbidden zone between the highest filled band and the lowest empty band is called the band gap, playing a major role in the optical and electric properties of the solid. Defects in the structure can lead to energy levels within the band gap. Examples are vacancies, or transient defects like exciton, which is a bound electron-hole pair. There are many different types of imperfections which may be caused by various processes. Mostly it depends on the growth process of the crystal or sometimes the manufacturing process, which will also determine the type of defect which will dominate the nature of the crystal. Unlike the bands which extend throughout the crystal, the additional levels are localized at the crystal defects, the energy levels introduced may be discrete energy levels, or may be distributed, depending on the exact nature of the defect and the nature of the host lattice.

Here we will consider defects caused by the introduction of foreign atoms into the crystalline structure. The ionization energy of the impurity ion (relative to the vacuum level) is changed drastically when it is placed within a lattice. Moreover, the electric field of the neighboring ions (crystal field) will remove partly or entirely the degeneracy of electronic orbits. Many of the important properties of insulators

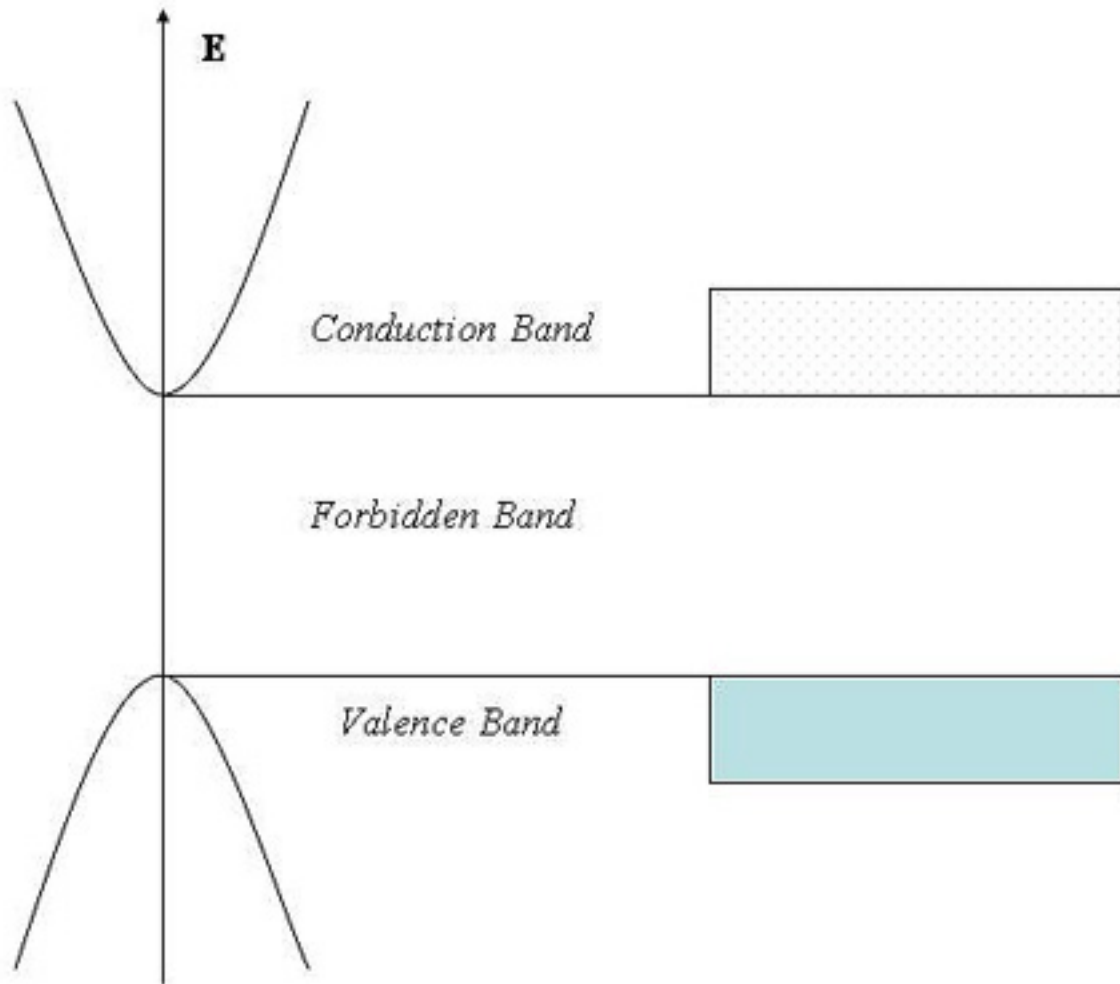


Figure 2.1: Band Structure [Shigeo Shionoya, W. M. Yen; *Phosphor Handbook*]

and semiconductors depend on additional energy levels which are associated with crystal imperfections. For example, silicon used in photocells or computer chips is heavily doped with impurities that can be thermally ionized at room temperature. For optical materials, one of the consequences of doping is the generation of new optical absorption bands, often giving the crystal a colored appearance. As an example,  $\text{Al}_2\text{O}_3:\text{Cr}^{3+}$  (ruby), pink ruby consists of  $\text{Al}_2\text{O}_3$  (sapphire) in which about 0.1% of the  $\text{Al}^{3+}$  ions are replaced by  $\text{Cr}^{3+}$  ions. In this case the sapphire is called the host material and the  $\text{Cr}^{3+}$  ions are dopants. [6].

### 2.3 PHOTOIONIZATION AND CHARGE TRANSFER

Electron transfer processes are defined here as charge transport between an impurity ion and the host valence or conduction bands and the band-to-band excitation that generates electron hole pairs. Traditionally, the transfer of an electron from the valence band to the impurity is called a charge transfer process. The promotion of an impurity electron into the host conduction band is called photoionization. The latter process is sometimes called metal-to-metal charge transfer process. In terms of a semiconductor picture, photoionization corresponds to a donor process and charge transfer to an acceptor process.

These three processes are shown in Fig. 2.2. Transition (a) corresponds to a band-to-band excitation, that occurs for photon energies  $h\nu \geq E_{Gap}$ .

Transition (b) corresponds to the photo-ionization of an impurity ion, producing an electron in the conduction band and an oxidized ion.

Transition (c) corresponds to a charge transfer process: the promotion of an electron from the valence band to an impurity ion, producing a free hole in the valence band and a reduced ion.

Electrons and holes generated in these processes can migrate within the lattice until they recombine (Fig. 2.3, d,e, and f). Another possibility is the capture of the carriers by electron or hole traps, a process that will be of utmost importance for our studies.

Traps can be classified as deep or shallow traps, where deep and shallow are not absolute characteristics, but describe the depth of a trap relative to  $kT$  at a given temperature.

So far all the discussion about electron transfer processes are concerned with transitions involving the delocalized bands. For example, in Figure 2.3, transition (f) involves relaxation of an electron from the conduction band to the impurity ion. In most relevant cases, however, the relaxation process will include the occupation of an excited impurity level, followed by impurity specific luminescence to the ground state (transition (j), Fig. 2.4). Similar transitions can be applied to holes.

The rare earths are good examples of substances which exhibit transition (j), Fig. 2.4. The rare earth ions are characterized by an incompletely filled 4f shell. The incomplete 4f shell in the rare earth ions results in a large number of well-defined luminescence emission lines. The 4f electron orbitals are shielded from the surroundings by the filled  $5s^2$  and  $5p^6$  orbitals[8]. The 4f states are thus not affected much by the surrounding host ions and therefore the spectra of the emission for the rare earths remain basically invariant in most host lattices.

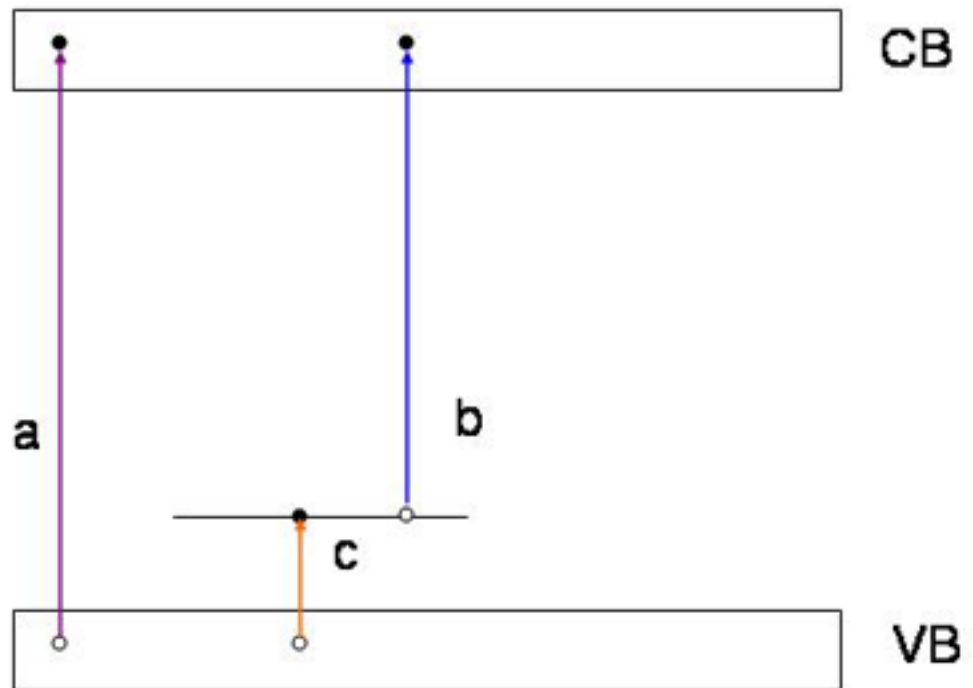


Figure 2.2: Electron transitions in insulators:(a) band to band excitation; (b)photoionization; (c)charge transfer; Electrons, solid circles; holes, open circles.

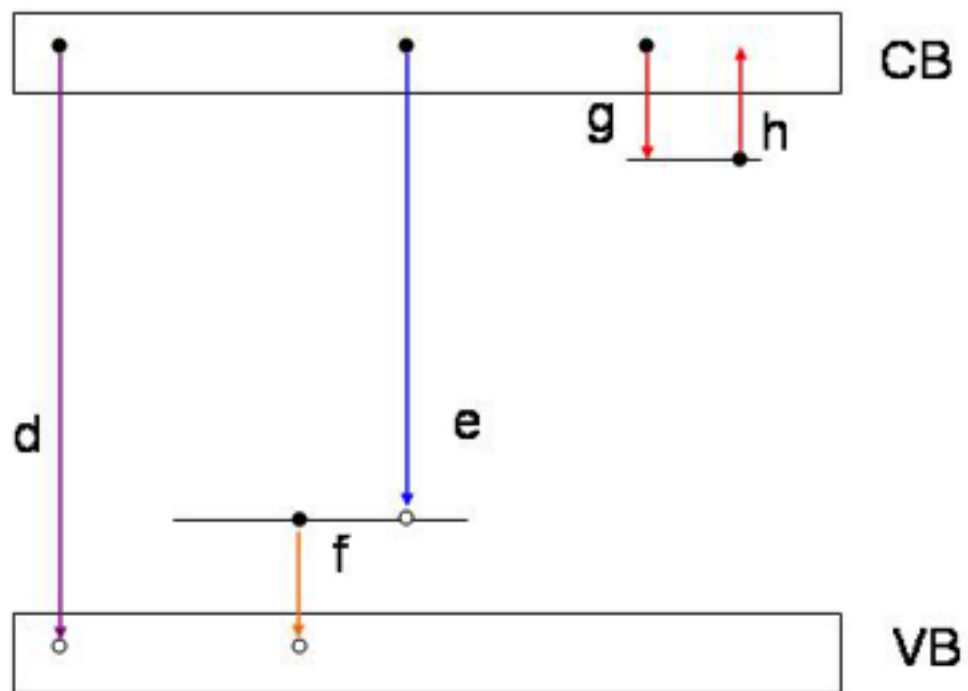


Figure 2.3: Electron transitions in insulators:(d) (e) and (f) are radiative or nonradiative relaxation. (g) trapping (h) untrapping ;Electrons, solid circles; holes, open circles.

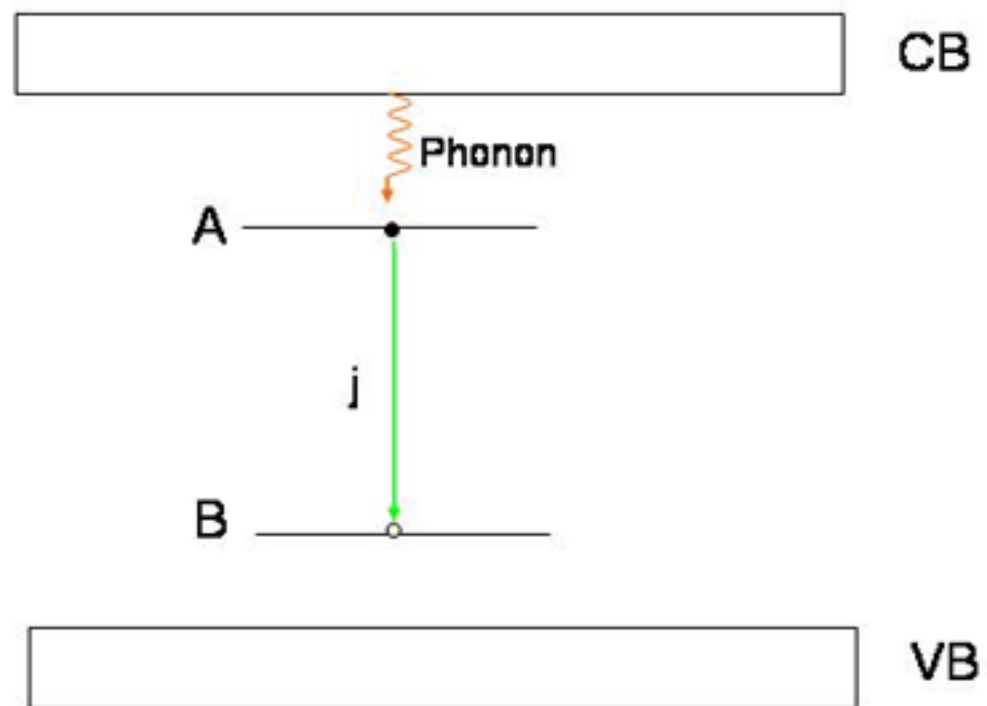


Figure 2.4: Electron transitions not involving the conduction or valence bands. Electrons-solid circles; Holes-open circles

## CHAPTER 3

### THEORY OF THERMOLUMINESCENCE

#### 3.1 LUMINESCENCE

The luminescence phenomena can be classified on the basis of various features. Historically these phenomena were separated according to the life time of the excited states - fluorescence with shorter life time and phosphorescence with longer life time. Blasse [8] defines fluorescence as spin-allowed transitions and phosphorescence as spin-forbidden transitions. If the selection rules are relaxed, the above definition becomes less practical.

Here we define the difference between fluorescence and phosphorescence according to the presence or absence of traps, although we must mention that Blasse classifies luminescence processes involving traps as *afterglow*.

Fluorescence and phosphorescence are schematically shown in Fig. 3.1: Fluorescence involves the spontaneous relaxation of an excited ion Fig. (3.1a), while for phosphorescence metastable energy levels are involved (shown in Fig. 3.1 (b)), where the electrons get trapped, and then return to the emitting state due to some additional energy (normally thermal).

#### 3.2 PHOSPHORESCENCE

The depth of the traps involved in the phosphorescence process is important for the duration of the emission. If the trapping into level  $m$  (metastable energy level) (Fig. 3.1) occurs at a temperature  $T$ , where the energy between these levels of  $m$

and  $e$ (excited state) is on the order of several  $kT$  (here  $k$  is Boltzmann's constant), then the electron will be more likely remain in the metastable level  $m$  for a long time, because the probability  $P$  per unit time for thermal excitation from the trap is exponentially dependent on temperature according to

$$P = s \cdot e^{-\Delta E/kT} \quad (3.1)$$

where  $s$  is a constant, with dimensions of reciprocal of time and  $\Delta E$  is the energy difference between the meta-stable level and the excited state. Thus, the time between excitation and final relaxation back to the ground state is delayed by the electron capture process.

The trap depth  $\Delta E$  is an important factor for understanding the phenomena of phosphorescence. Assuming that we excited the system with a constant intensity that is removed, we find, by following Randall and Wilkins [9], that the rate of thermal excitation of electrons from level  $m$  back to the excited state  $e$  is given by:

$$-\frac{dn}{dt} = np = n \cdot s \cdot e^{-\Delta E/kT} \quad (3.2)$$

where the negative sign indicates the loss of electrons. Assume that there is no re-trapping process for the electrons to fall back into level  $m$ , the intensity  $I$  of the luminescence which results from the decay of the electron from excited state  $e$  to the ground state  $g$  is given by the de-trapping rate via the  $m \rightarrow e$  transitions and thus:

$$I(t) = -\eta \frac{dn}{dt} = \eta \cdot n \cdot s \cdot e^{-\Delta E/kT} \quad (3.3)$$

where  $\eta$  is a constant. After integration we find

$$I(t) = I_0 e^{-tp} \quad (3.4)$$

where  $I_0$  is the initial intensity at  $t=0$ . The phosphorescence decay under these circumstances then can be represented by a simple exponential function of time, where the decay rate  $p$  depends on  $\Delta E$  and  $T$  according to Eq. 3.1.

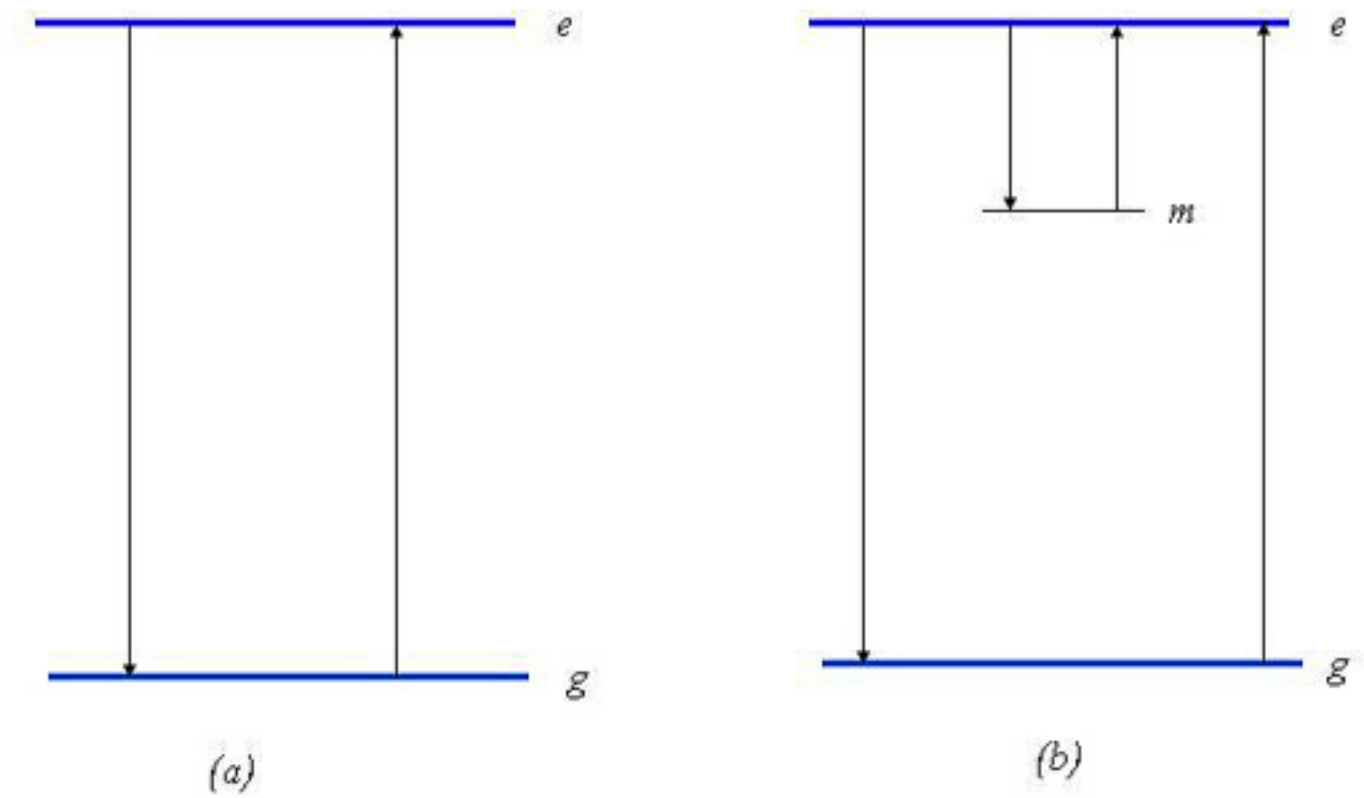


Figure 3.1: (a) Excited state  $e$  and ground state  $g$  energy levels showing absorption and emission for the process of fluorescence. (b) Metastable level  $m$  giving rise to a delay between excitation and emission during the process of phosphorescence.

### 3.3 THERMOLUMINESCENCE

Thermoluminescence, or thermally stimulated luminescence (TSL) is a temperature-stimulated light emission. Thermoluminescence is a special case of phosphorescence observed under the condition of increasing temperature. In the TSL experiments, the system is illuminated at a constant (usually low) temperature to meet the condition that  $kT < \Delta E$ . thus, the electrons will remain trapped during the illumination phase. The illumination is followed by a heating process with constant rate, which will deplete the traps with previously stored electrons, resulting in the emission of luminescence.

The luminescence intensity recorded as a function of temperature is called a glow-curve. Fig 3.2 shows an experimental example obtained for  $\text{Sr}_2\text{SiO}_4:\text{Eu}^{2+}$ . In this case two peaks can be seen, corresponding to two traps with different trap depth: the higher the temperature needed to empty the trap the deeper the trap is. The maxima of the glow-curves are called glow-peaks and can be used to study the trap structure of a solid. Efficient thermoluminescent materials have a high concentration of electron and hole traps, provided by structure defects and impurities as discussed previously.

Schematically, the TSL process is shown in Fig. 3.3, with the illumination and trap filling phase shown as process (a), and the thermally stimulated de-trapping phase shown as process (b). The light emitted by the un-trapped electrons that recombine with the electron donors is called thermoluminescence.

### 3.4 GLOW CURVE ANALYSIS

Before we derive the differential equations that describe the glow-curve, we will qualitatively analyze the thermoluminescence process (Fig. 3.5). The top shows the probability of the untrapping process as a function of temperature. At very low

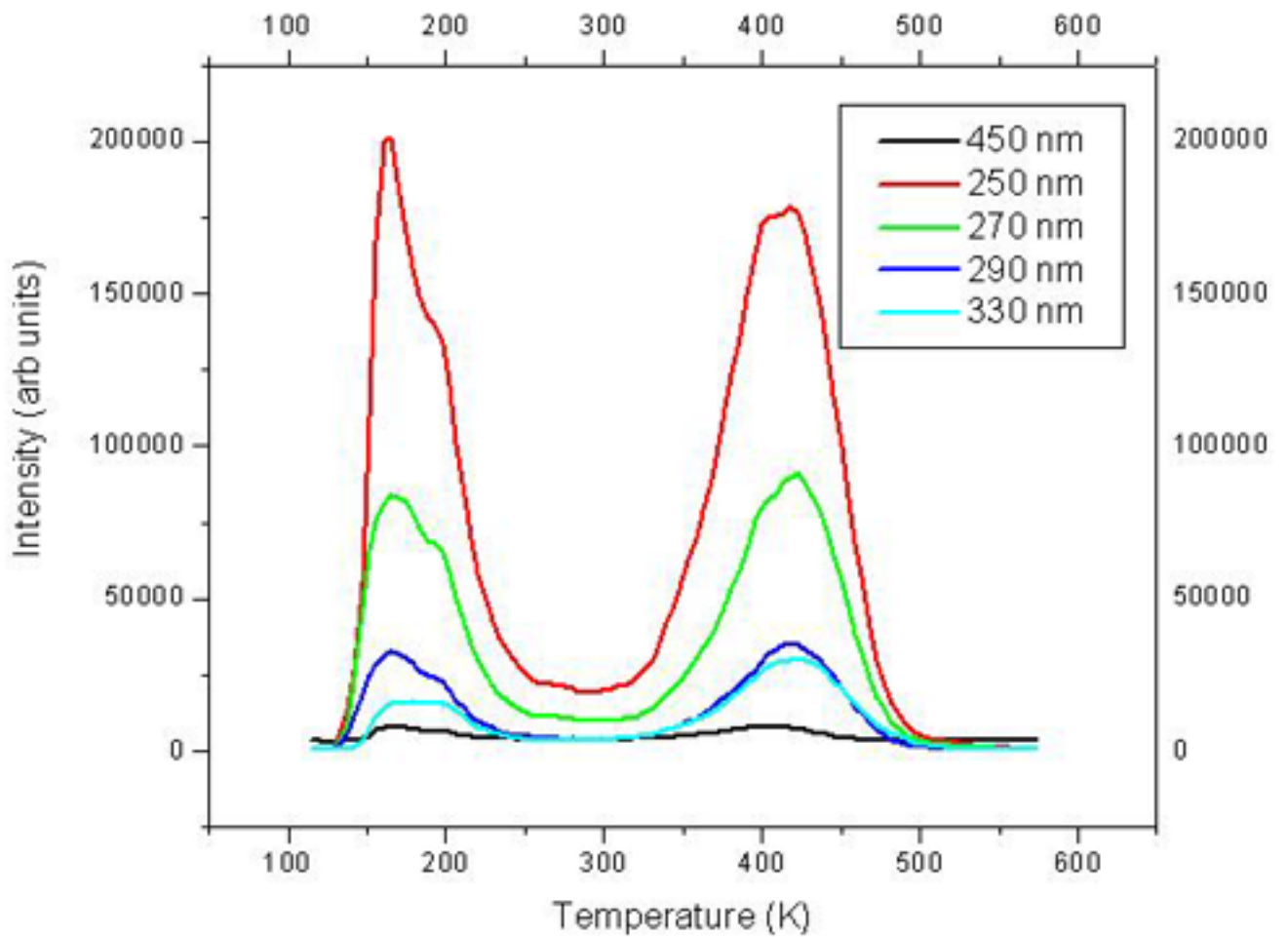


Figure 3.2: Typical thermally stimulated luminescence glow curve of  $\text{Sr}_2(\text{SiO}_4):\text{Eu}^{2+}$ , there are two peaks corresponding to different trap depth.

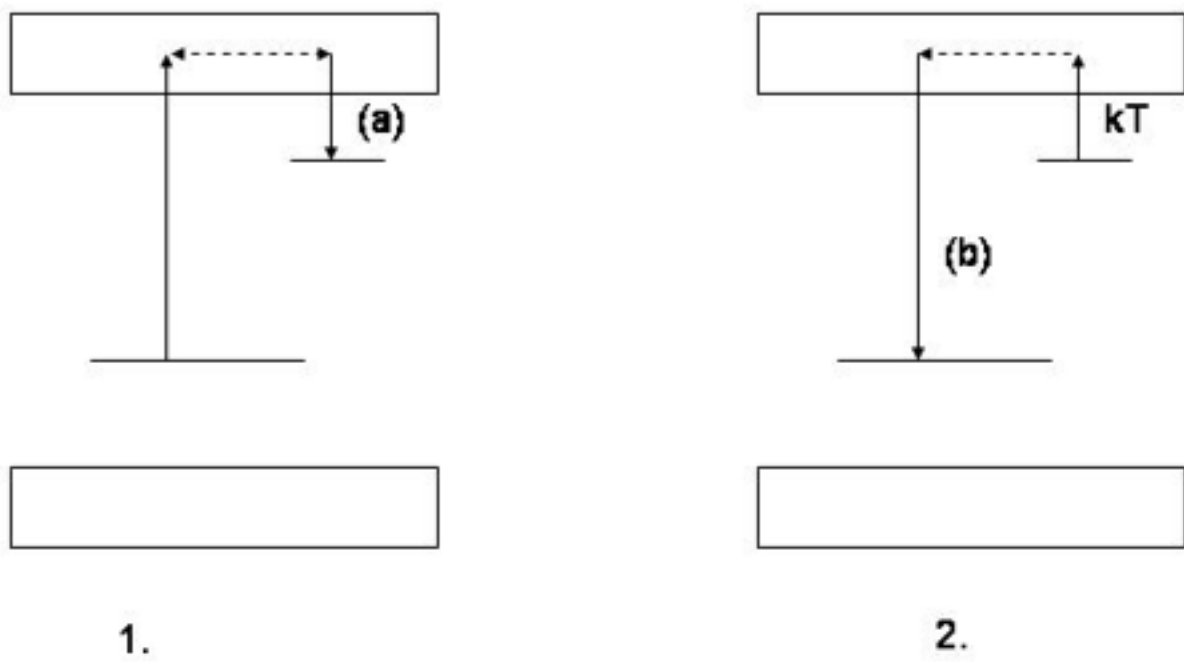


Figure 3.3: Processes produced in the crystalline structure by irradiation and by heating

temperatures the probability for the trapped electrons to escape is vanishingly small, because the electrons do not have enough thermal energy to escape from the trap. As the temperature increases the probability for these charge carriers to escape will increase, along with the temperature increase the probability usually goes from 0 to 1 integrated over time (see Eq. 3.1). During this process the charge carriers find their way to the recombination centers which usually are the ground states of the centers and emit light. During this period, the trapped charge population is decreasing monotonically. The luminescence intensity (given by the derivative of the trapped charge population) goes through a maxima during the trap emptying process. The feature of the glow curve here is not dependant on the properties of the recombination centers, but purely due to the release of the charge carriers from the traps. If the crystal contains more than one type of trap, the glow curve will be characterized by the temperature of the maximum intensity,  $T$ , the activation energy,  $\Delta E$ , and a pre-exponential factor  $s$  with units of inverse seconds.

Quantitatively, this mechanism can be described by a first - order (no re-trapping) kinetic equation. For the de-trapping rate we have

$$\frac{dn}{dt} = -n \cdot s \cdot e^{-\Delta/kt} \quad (3.11)$$

where  $n$  is the trapped charge population,  $k$  is Boltzmann's constant and  $T$  is the temperature. This is based on the assumption that the fraction of released charges reaching the luminescence center is independent of time or temperature, i.e. the thermoluminescence intensity  $I_{TL}$  can be assumed proportional to  $dn/dt$ :

$$I_{TL} = -\frac{dn}{dt} = n \cdot s \cdot e^{-\Delta/kT} \quad (3.12)$$

For a linear heating rate,  $T = \beta t$ , the solution of Equation 3.11 is

$$n = n_0 e^{-\int_0^T (s/\beta) e^{(-\Delta E/kT)} dT} \quad (3.13)$$

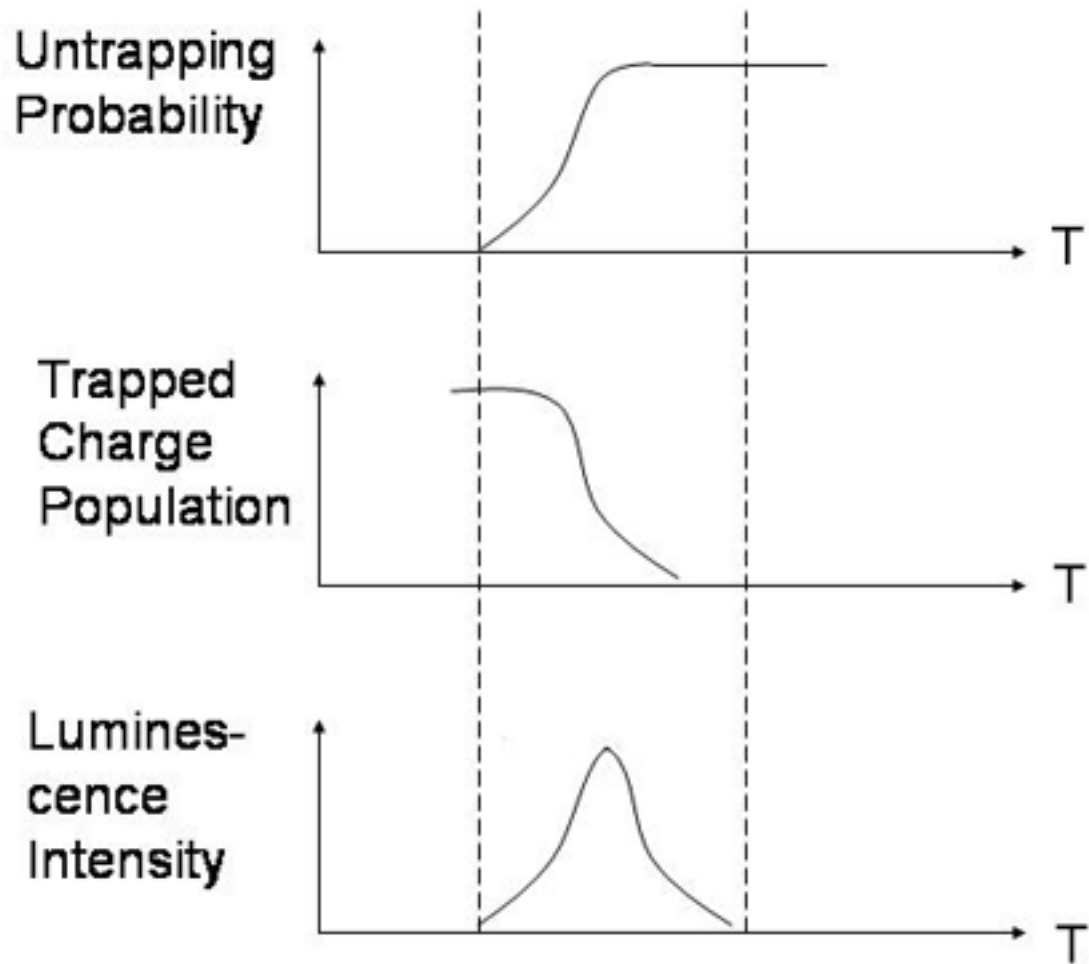


Figure 3.4: The relation between the untrapping probability, luminescent intensity, and trapped charge population.

$$I_{TL} = n_0 \cdot s \cdot e^{-\Delta E/kT} e^{-\int_0^T (s/\beta) e^{-\Delta E/kT} dT} \quad (3.13)$$

$I_{TL}$  is the thermoluminescence intensity.

## CHAPTER 4

### THERMOLUMINESCENCE EXPERIMENT

#### 4.1 THERMALLY STIMULATED LUMINESCENCE EXCITATION SPECTROSCOPY (TSLES)

Thermoluminescence can be used to determine the energy threshold for promoting electrons from impurities to the conduction band or holes to valence band. The basic idea is simple: the integrated glow-curve intensity is proportional to the number of trapped carriers during illumination. If the photon energy of the light is insufficient to promote carriers into the host bands, no TSL signal will be obtained. If we repeat the TSL experiment several times with increasingly higher photon energy, a TSL signal will be observed when the photon energy reaches the threshold for ionization or charge transfer. Thus, by plotting the integrated glow-curve intensity versus the photon energy used for illumination, the ionization or charge transfer energy can be conveniently obtained. This method can be called Thermally Stimulated Luminescence Excitation Spectroscopy (TSLES), because it is a form of excitation spectroscopy that probes the promotion of impurity electrons into the conduction band or holes into the valence band.

The simple concept is reflected in the rather straightforward experiments. The sample is mounted in a cryostat that can be heated to high temperatures. First, the sample is heated to high temperatures without illumination in order to empty all traps (sample "reset"). The sample is then cooled down to the base temperature of the cryostat and illuminated for a certain period of time with monochromatic

light. After the illumination process, the sample is heated at a constant rate, and the thermoluminescence is recorded as a function of temperature. Thus, for each wavelength of the incident light there will be a corresponding glow curve, and by integrating the area under each glow curve an excitation spectrum can be obtained by plotting the integrated glow curve as a function of wavelength (shown in Figure 4.2). The excitation spectrum will show a signal onset at a photon energy that corresponds to the photo-ionization or charge transfer energy.

## 4.2 EXPERIMENTAL EQUIPMENT AND SETUP

### Experiment setup

The thermoluminescence obtained depends on the samples that need to be investigated. Common are the three basic components: a cryostat equipped with a heater, a tunable excitation source, and a luminescence detection system.

## 4.3 TYPICAL CRYOSTAT DESIGN

The cryostat needed for recording the signal has to be able to work as a furnace. Some of the samples investigated in our group are heated to 600 °C. In order to heat the sample and record the temperature, electrical feed-through is necessary. In order to minimize the experimental time, the cryostats built in our laboratory are very small which to ensure rapid cool-down times.

A schematic TSL cryostat is shown in Fig. 4.3. It is of a single window design, where one opening is used for both excitation and detection of the thermoluminescence. If powdered samples are used, a second window is used to press the material onto the cryostat cold finger, and one has to take care that the window does not contribute to the TSL signal. Usually a UV grade fused quartz is used in our laboratory.

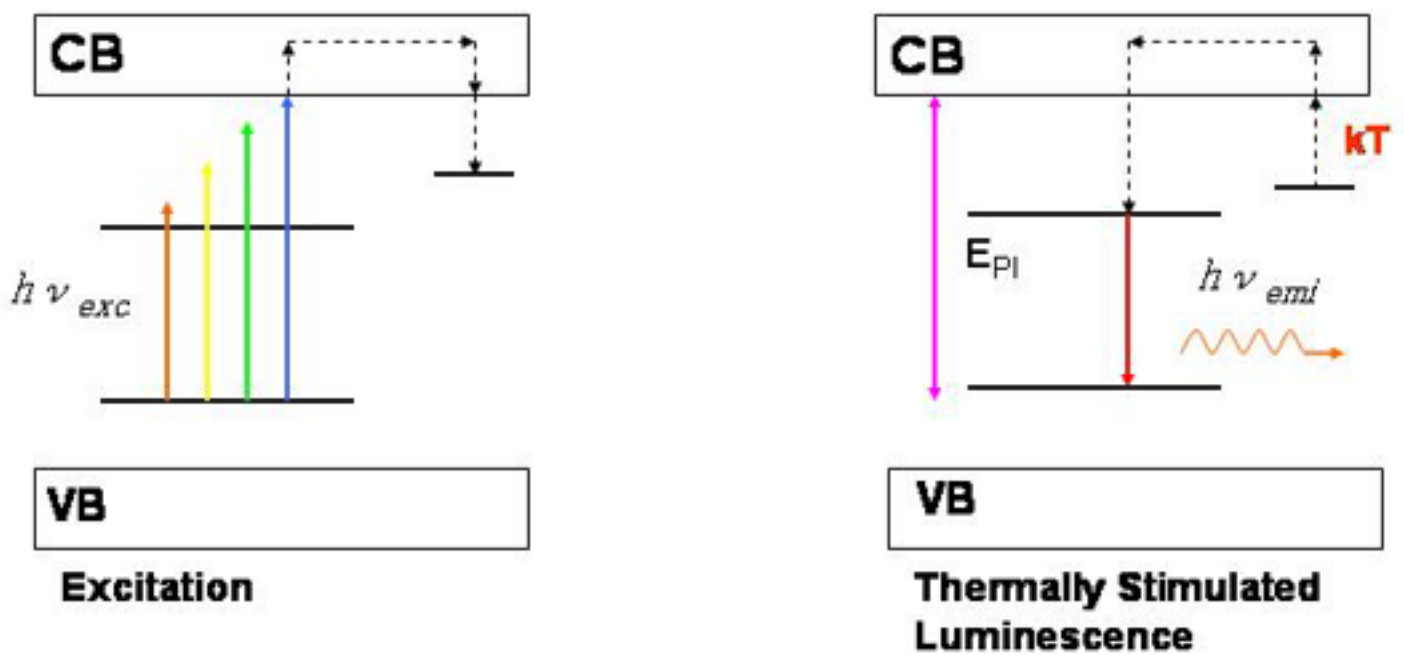


Figure 4.1: The Principle of using TSL to locate the ground state of an impurity. Thermoluminescence spectroscopy determines the onset of trap filling which gives the ionization energy  $E_{PI}$ .

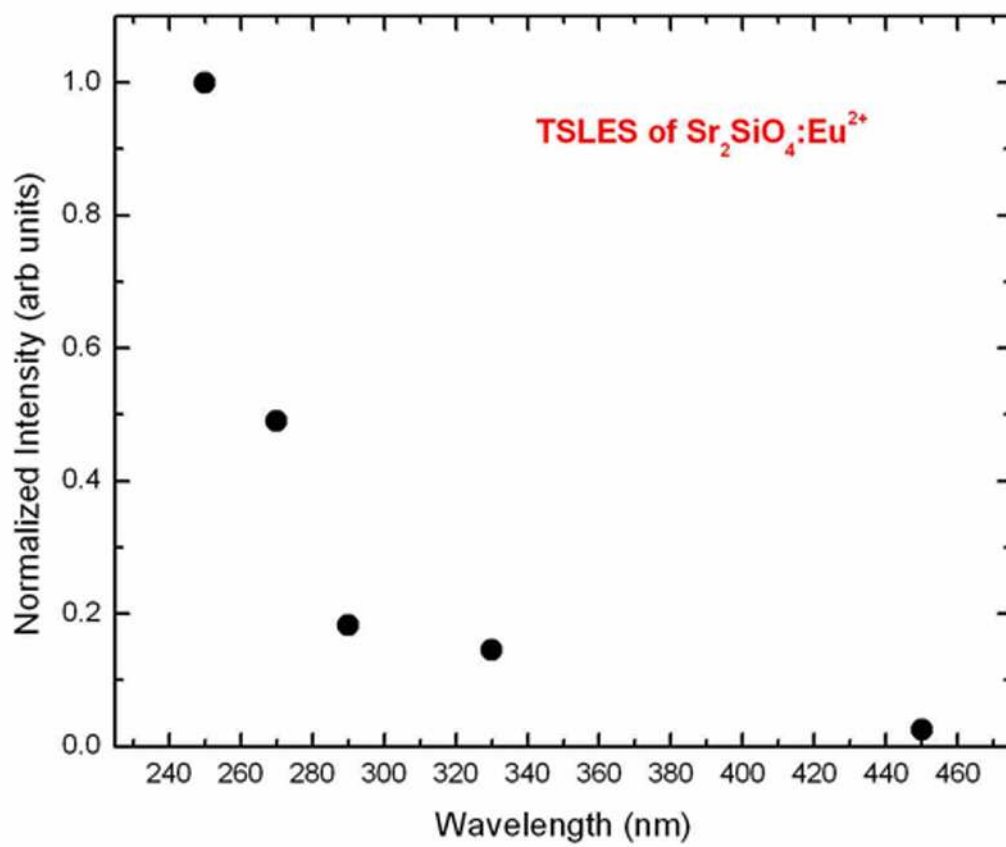


Figure 4.2: A Thermally Stimulated Luminescence Excitation Spectroscopy TSLES; plotted data is the TSLES of  $\text{Sr}_2\text{SiO}_4:\text{Eu}^{2+}$

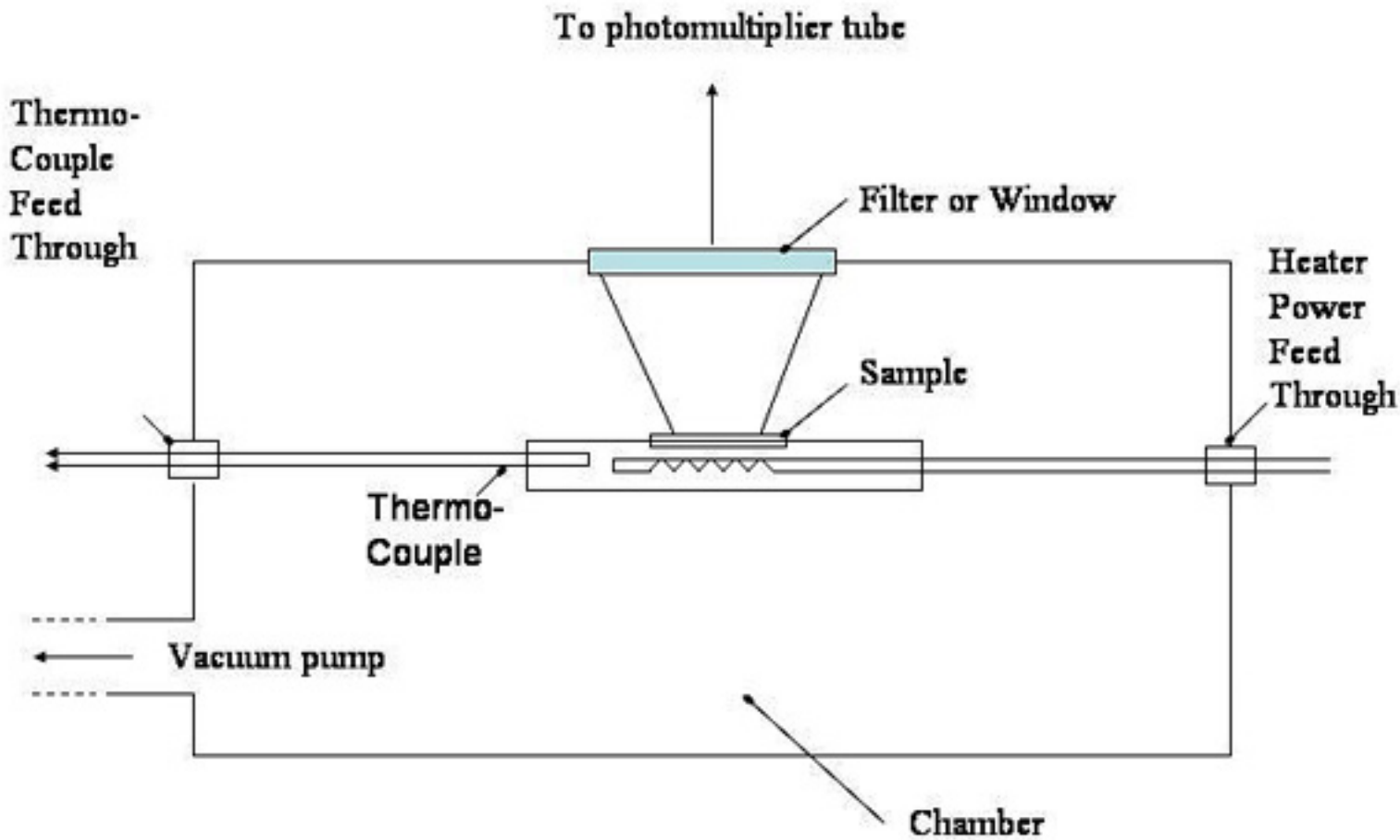


Figure 4.3: Typical design for a sample chamber for recording thermoluminescence.[S.W.S. McKeever ; *Thermoluminescence of Solids*]

### 4.3.1 CRYOSTAT USED FOR THE $\text{Sr}(\text{SCN})_2:\text{Eu}^{2+}$ EXPERIMENTS

The  $\text{Sr}(\text{SCN})_2:\text{Eu}^{2+}$  sample investigated in this thesis required a departure from the standard nitrogen cold finger cryostat used in TSL measurements. This sample shows strong thermal quenching, starting around 100 K, with the luminescence completely quenched around 200 K. Thus we used a commercial CF1204 Oxford flow-through cryostat, with a base temperature of about 4 K. Having indium sealed inner windows, the cryostat can be heated to room temperature only, but this is not a drawback in this case, because the luminescence is already quenched at the temperature of 200K. A cross-section through the cryostat is shown in Fig. 4.4.

This cryostat has a built-in heater and a controller to ramp the temperature linearly.

### 4.3.2 THE EXPERIMENTAL SETUP

The experiment setup is shown in fig 4.5. A 100 W Xenon lamp is used as a tunable light source for this experiment, in conjunction with interference filters which have a bandwidth of 10 nm Full Width Half Maximum (FWHM). A BG-28 cut-off filter is used to reduce the heat load on the interference filters. The light is focused through a quartz lens onto the sample, which is located in the cryostat sample chamber, immersed in helium gas.

Thermoluminescence is detected with a bialkali Hamamatsu Photomultiplier (PMT), connected to a fast discriminator. The discriminator signal is recorded with a multichannel scaler (EG&G ) controlled by a computer.

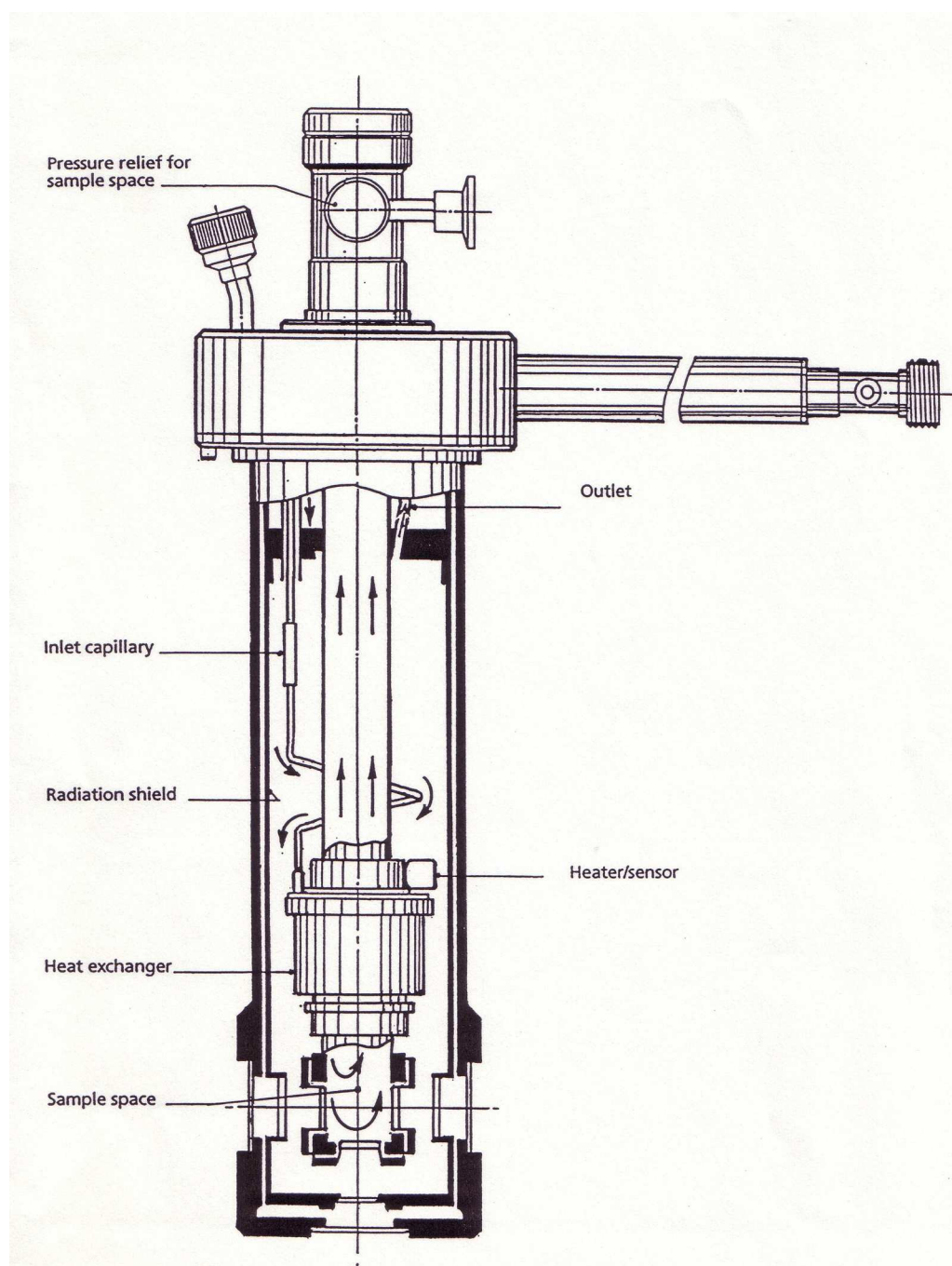


Figure 4.4: CF1204 Continuous Flow Cryostat made by Oxford Instruments used in this experiment [Oxford Instrument; *CF1204 Cryostat Handbook*].

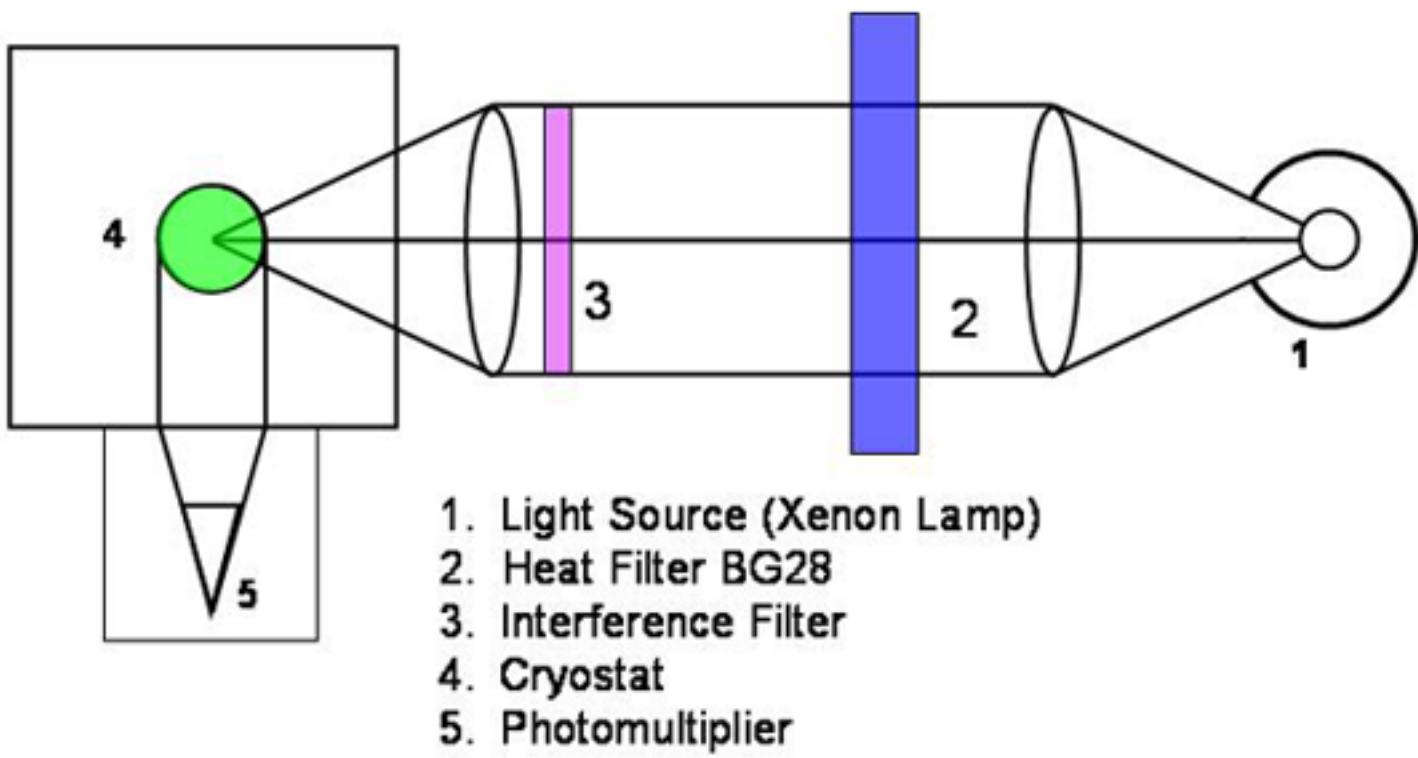


Figure 4.5: Experimental Setup

### 4.3.3 $\text{Sr}(\text{SCN})_2:\text{Eu}^{2+}$ (STRONTIUM THIOCYANATES DOPED WITH EUROPIUM 2+)

The sample measured in this thesis is  $\text{Sr}(\text{SCN})_2:\text{Eu}^{2+}$  and was prepared by Dr. Claudia Wickleder, Institut für Anorganische Chemie, Universität Siegen, Germany.

Dr. Wickleder has described the properties of the host material in detail, as well as the luminescence of  $\text{Eu}^{2+}$  doped samples [11][13][12]. The crystal structure of the material is shown in Fig. 4.9.  $\text{Eu}^{2+}$  ions substitute for Sr ions. This material is of interest due to the strong covalent binding character due to the SCN groups. Dr. Wickleder requested a measurement of the ionization threshold for the  $\text{Eu}^{2+}$  ions in  $\text{Sr}(\text{SCN})_2:\text{Eu}^{2+}$ , because the Eu luminescence quenches around 150 K (Fig. 4.6), and it was suspected that the quenching is due to photo-ionization. Level crossing, a quenching mechanism that is often observed, was unlikely due to the small Stokes shift of the d-f emission [6].

As mentioned above, the thermal quenching required the use of a helium cryostat to illuminate the sample far below the onset of thermal quenching, and it was hoped that sufficiently shallow traps existed in order to record a TSL signal. The sample is also very hygroscopic and had to be sealed in a quartz vial, which makes TSLES a technique that is superior to the alternative method of photoconductivity in this case. In order to provide proper heat exchange, the vial was filled with argon gas.

$\text{Sr}(\text{SCN})_2:\text{Eu}^{2+}$ 's emission strength is strongly dependent on temperature, the sample glows bright green at low temperature, and as the temperature increases the intensity of light emitted from the sample decreases rapidly above 130 K. The quenching of the luminescence intensity is reflected in a similar decrease of the luminescence decay time, as shown in Fig 4.11. The temperature dependence of life time measurements are shown in Fig 4.11. The lifetimes were obtained by irradiating the sample at a wavelength of 400 nm using a few nJ pulses of 3 nsec duration and

100 kHz repetition rate. The luminescence was recorded using a time-to amplitude converter (ORTEC) and a pulse height analyzer (EG&G).

Lifetime or intensity measurements cannot distinguish between photo-ionization or level crossing, but it will provide the energetic position of the quenching level relative to the Zero Phonon Line (ZPL), a value that will be compared later with the results of the TSLES measurements.

In order to distinguish between photo-ionization and level crossing, we performed TSLES measurements, the idea being that photo-ionization would lead to a TSL signal, while level crossing would not.

#### 4.3.4 ANALYSIS OF THE LUMINESCENCE QUENCHING

Before performing the TSLES experiments, one can estimate the location of the quenching conduction band from the temperature dependence of the  $\text{Eu}^{2+}$  luminescence and/or the relaxation time. The analysis of the quenching will provide the location of the quenching level relative to the ZPL. At this point, we do not specify the quenching mechanism, it can be level crossing or photoionization.

We used the Arrhenius model to find the quenching level, and obtained the curve shown in Fig. 4.11. The fit provided an energy of  $\Delta E=1400 \text{ cm}^{-1}$  for the quenching level with respect to the ZPL. Given a ZPL energy of  $21505 \text{ cm}^{-1}$ , the quenching level is located  $22905 \text{ cm}^{-1}$  above the  $\text{Eu}^{2+}$  ground state.

The Arrhenius model in its simplest form treats the quenching problem in a 3-level system (Fig. 4.9).

Provided that levels 1 and 2 are in thermal equilibrium, and that  $N_1$  and  $N_2$  are the populations of level 1 and level 2, respectively, the total relaxation rate to the ground state is given by the sum of the decay rates from level 1 and level 2. To adapt this simple model to our problem, we assume that the relaxation from level 1 represents the radiative d-f relaxation of the  $\text{Eu}^{2+}$  ion, and the relaxation from

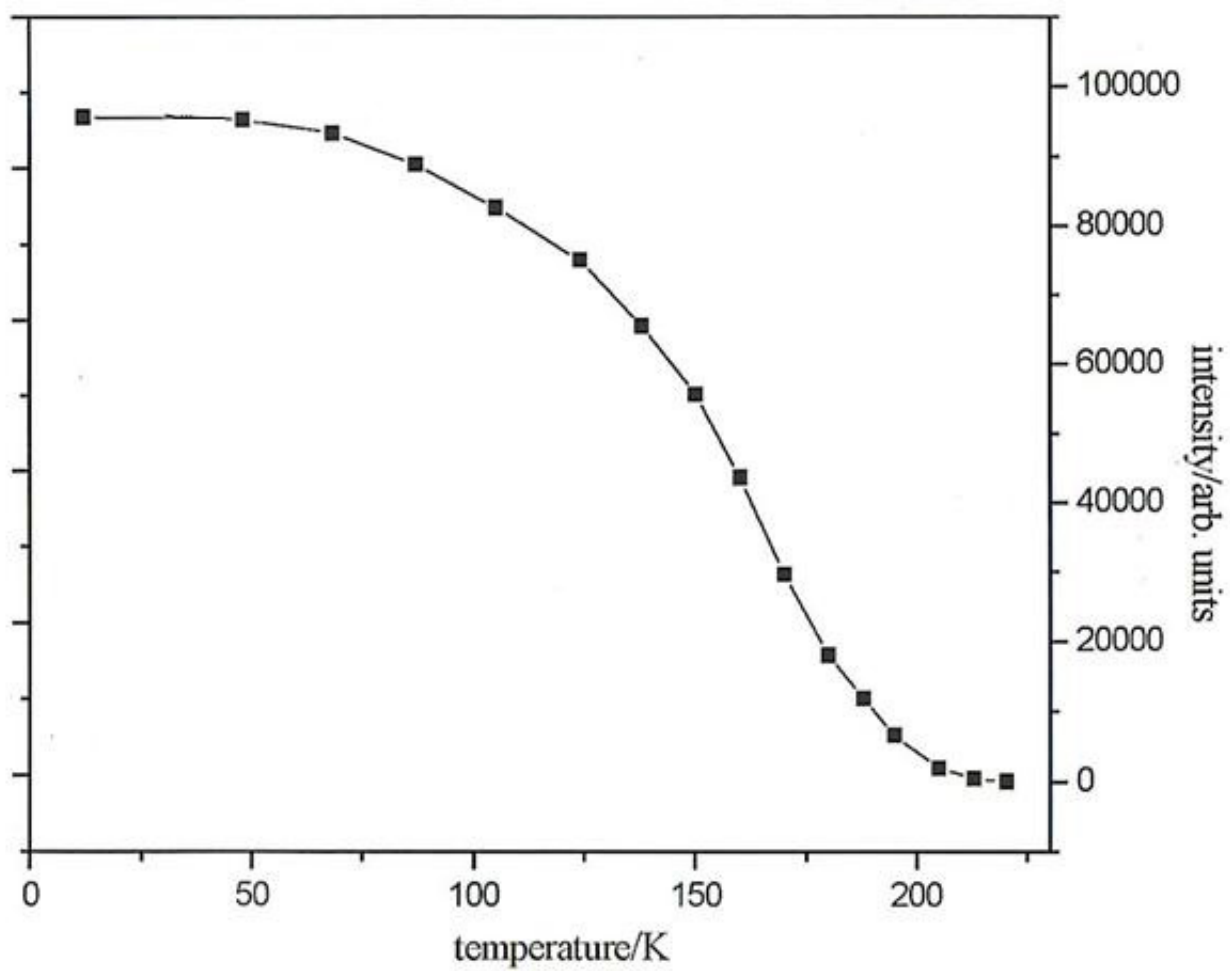


Figure 4.6: Temperature dependence of emission of Sr(SCN)<sub>2</sub>:Eu<sup>2+</sup> [From Dr. Wickleder C.]

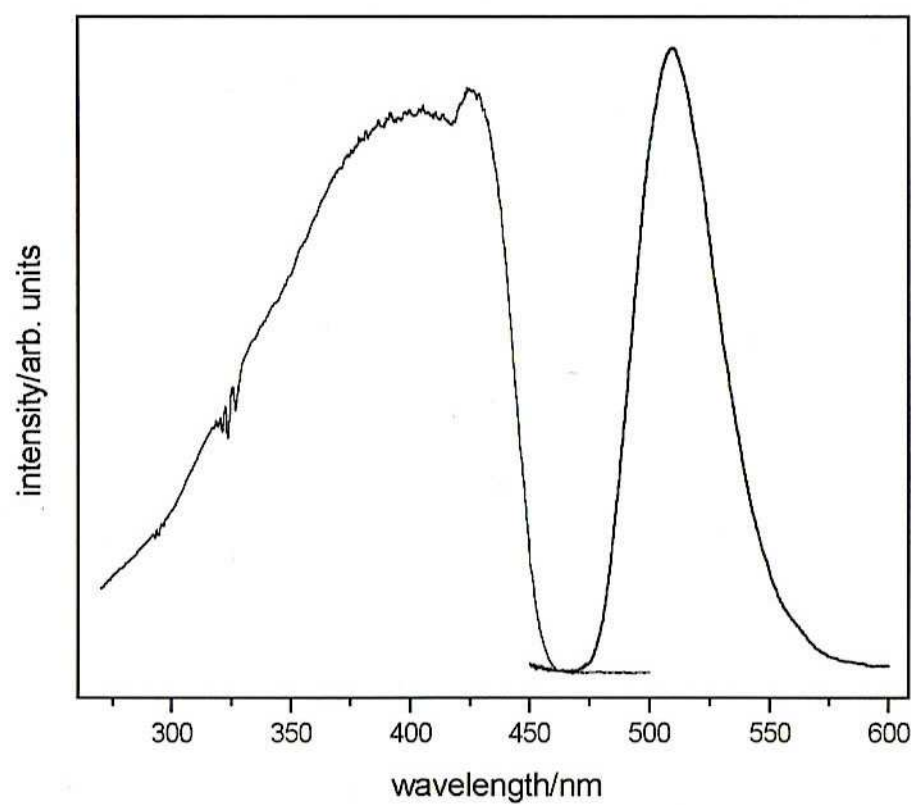


Figure 4.7: Excitation and emission spectrum of Sr(SCN)<sub>2</sub>:Eu<sup>2+</sup> [From Dr. Wickleder C.]

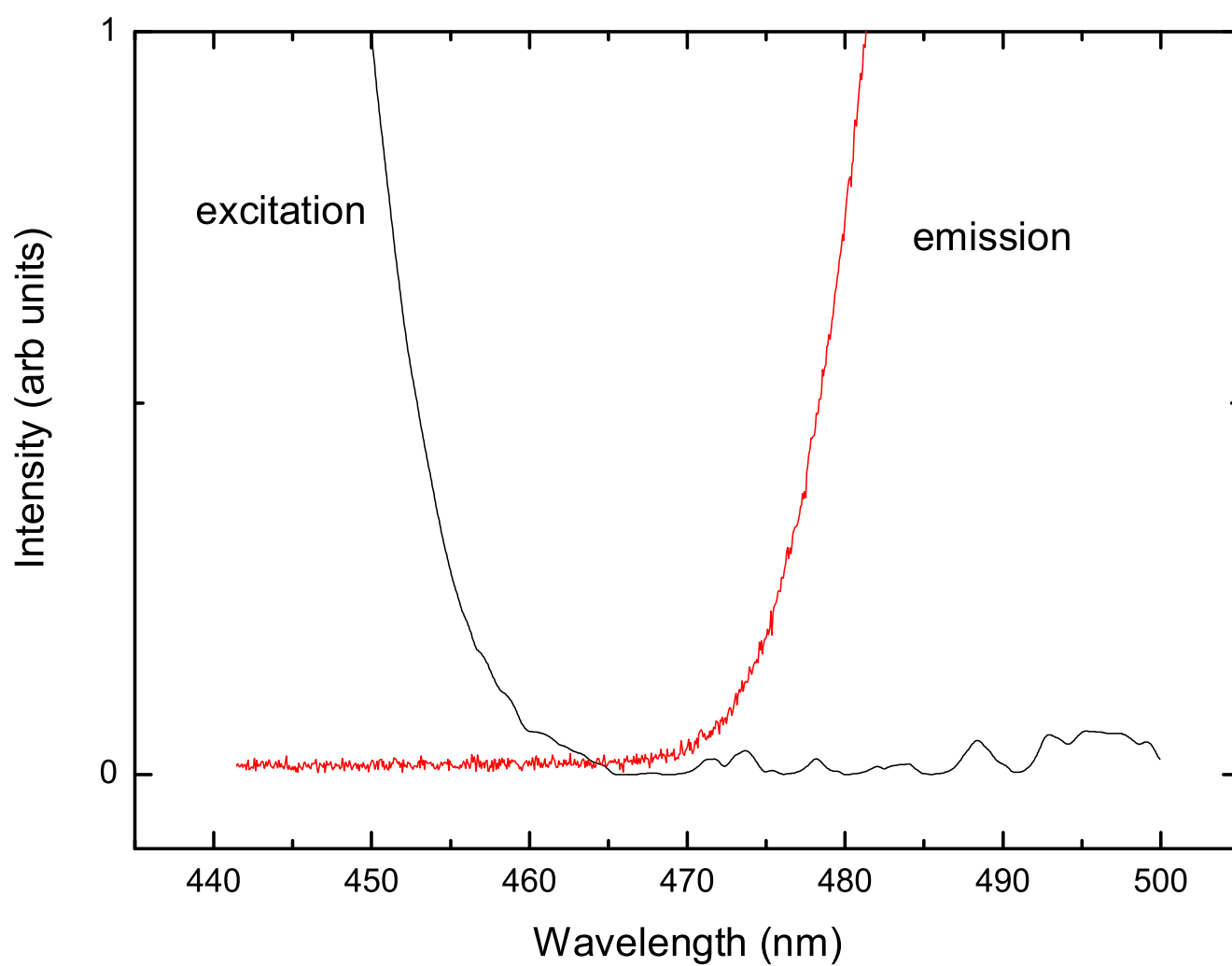


Figure 4.8: The emission and excitation of  $\text{Sr}(\text{SCN})_2:\text{Eu}^{2+}$  measured in our lab. Shows ZPL is at 465 nm.

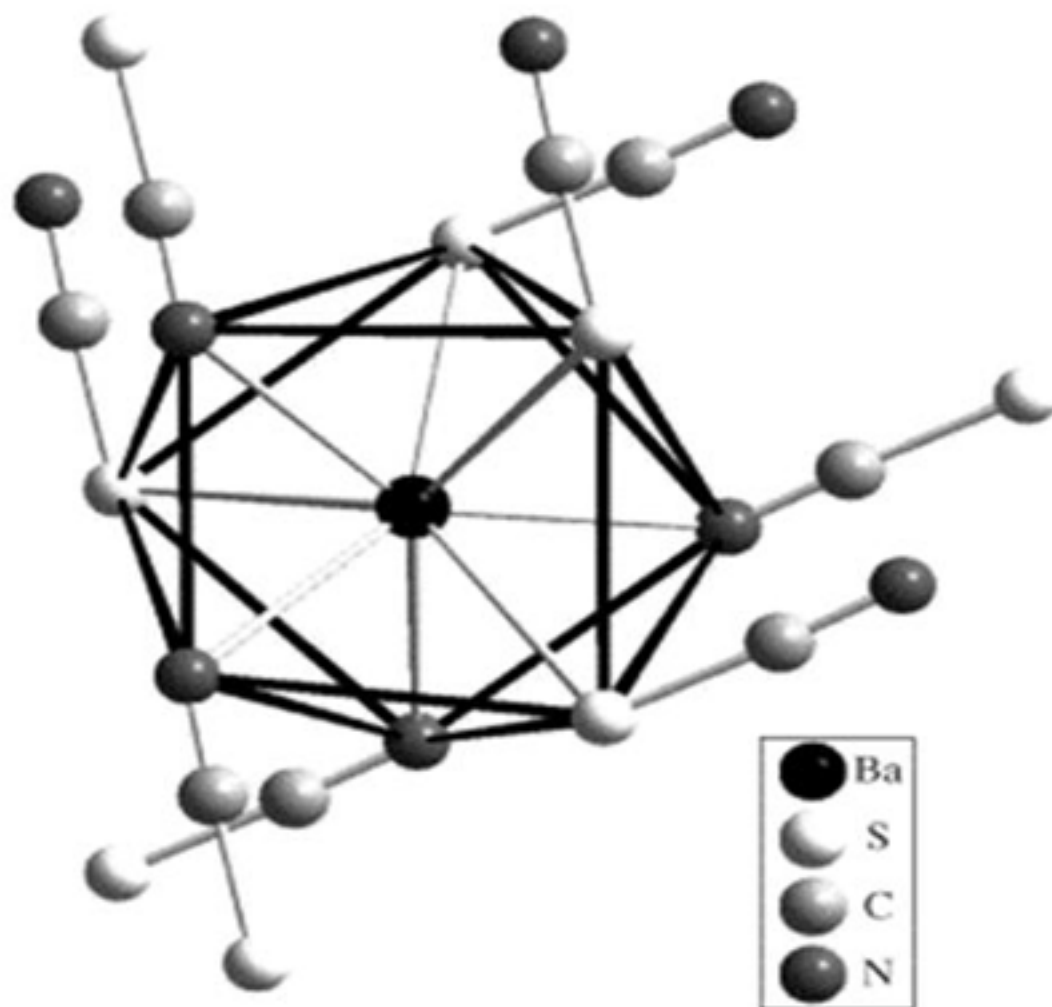


Figure 4.9: The crystal structure of Ba(SCN)<sub>2</sub>:Eu<sup>2+</sup>, Sr(SCN)<sub>2</sub>:Eu<sup>2+</sup> has similar structure [Dr. Wickleder C.; *J of Alloys and Compounds*,374(2004) 10-13]

level 2 represents the non-radiative relaxation from the quenching level. Using  $\Gamma_t$  to represent the total relaxation rate, we have

$$\Gamma_t = \Gamma_1 + \Gamma_2 \quad (4.1)$$

$$\Gamma = N/\tau \quad (4.2)$$

Here  $\tau$  is the life time of the emission after the excitation of the excited state. Assuming thermal equilibrium between the two excited levels the relationship between  $N_1$  and  $N_2$  is given by

$$N_2 = N_1 \cdot e^{-\Delta/kT} \quad (4.3)$$

Thus we have

$$N = N_1 + N_2 = N_1 + N_2 \quad (4.4)$$

then we have

$$N/\tau = N_1/\tau_1 + N_2/\tau_2 \quad (4.5)$$

Dividing by  $N_1$  we have

$$(1 + e^{-\Delta/kT})/\tau = 1/\tau_1 + e^{-\Delta/kT}/\tau_2 \quad (4.6)$$

and

$$\tau_t = \frac{1 + e^{-\Delta/kT}}{(1/\tau_1 + (1/\tau_2) \cdot e^{-\Delta/kT})} \quad (4.7)$$

Using this equation to fit the temperature dependence of the life time, we obtain the value  $\Delta=1400 \text{ cm}^{-1}$

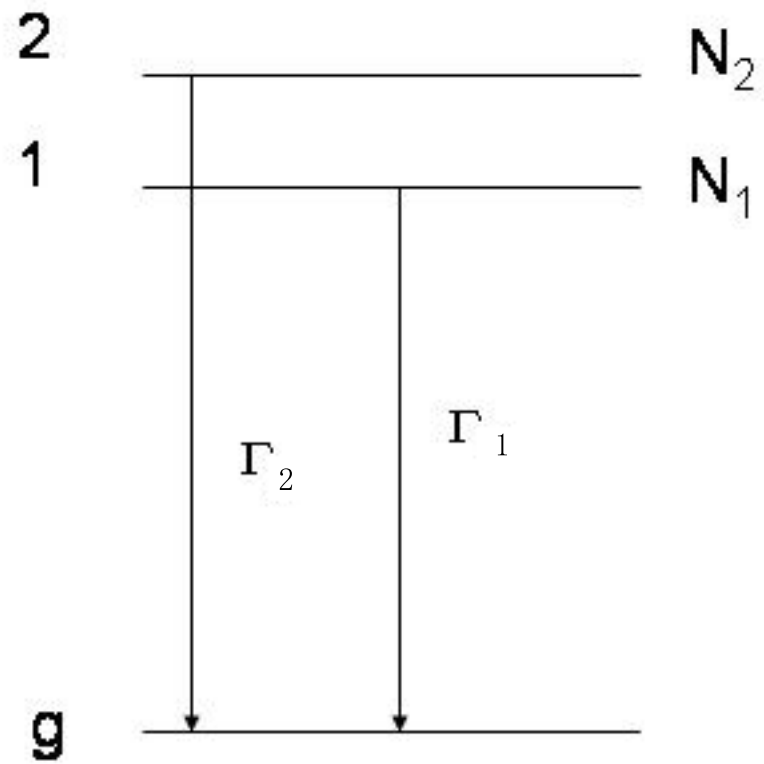


Figure 4.10: A simple two level system,  $N_1$  and  $N_2$  are the electron populations in the excited states

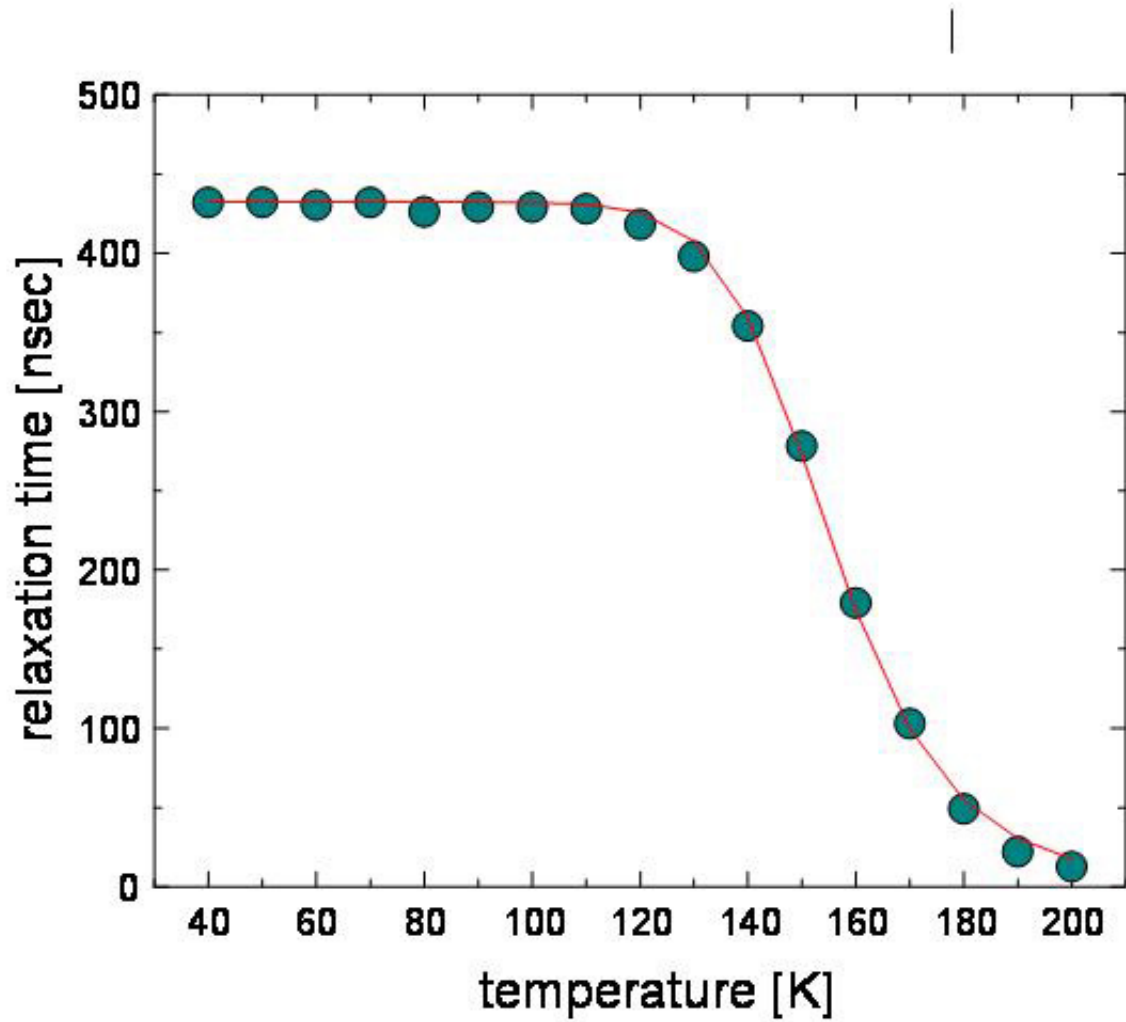


Figure 4.11: The temperature dependence of lifetime measurements of  $\text{Sr}(\text{SCN})_2:\text{Eu}^{2+}$

## 4.4 EXPERIMENT RESULTS

### 4.4.1 TSLES OF $\text{Eu}^{2+}$ IN $\text{Sr}(\text{SCN})_2$

The analysis of the glow curve provided an estimate of the quenching level, around  $1400 \text{ cm}^{-1}$  above the ZPL. Thus we could concentrate our TSLES measurements in the spectral range between 470 nm and 400 nm. The sample was cooled to 20K for illumination, and heated to room temperature during the recording of the glow curves. Glow curves corresponding to different excitation wavelengths are shown in Fig. 4.11. Three traps are evident in the plot, with the two dominant peaks in the 70 K to 120 K region.

Here we can draw our first important conclusion: the measured TSL signal provides evidence of a photo-ionization process. Thus we have confirmed the hypothesis that the quenching in  $\text{Sr}(\text{SCN})_2:\text{Eu}^{2+}$  is due to photo-ionization.

As expected, no TSL signal is found above 170 K: while deep traps probably do exist, the quenching of the luminescence at high temperatures prohibits their observation.

After the glow curves are collected, the area under each glow curve is integrated, and the integrated signal plotted as a function of the excitation wavelength.

The resulting spectrum of  $\text{Eu}^{2+}$  in  $\text{Sr}(\text{SCN})_2$  is presented in fig 4.13, where an obvious onset of the signal can be seen at 460 nm. Considering the spectral width of the filters used, the actual value of the ionization energy corresponds to a wavelength of 450 nm, or  $22222 \text{ cm}^{-1}$ . Comparing this to the position of the ZPL at 465 nm, we calculate the conduction band to be  $720 \text{ cm}^{-1}$  above the ZPL energy.

### 4.4.2 DISCUSSION

Our experiments have confirmed that the quenching in  $\text{Sr}(\text{SCN})_2:\text{Eu}^{2+}$  is due to photoionization. Comparing the ionization energy to the value obtained from the

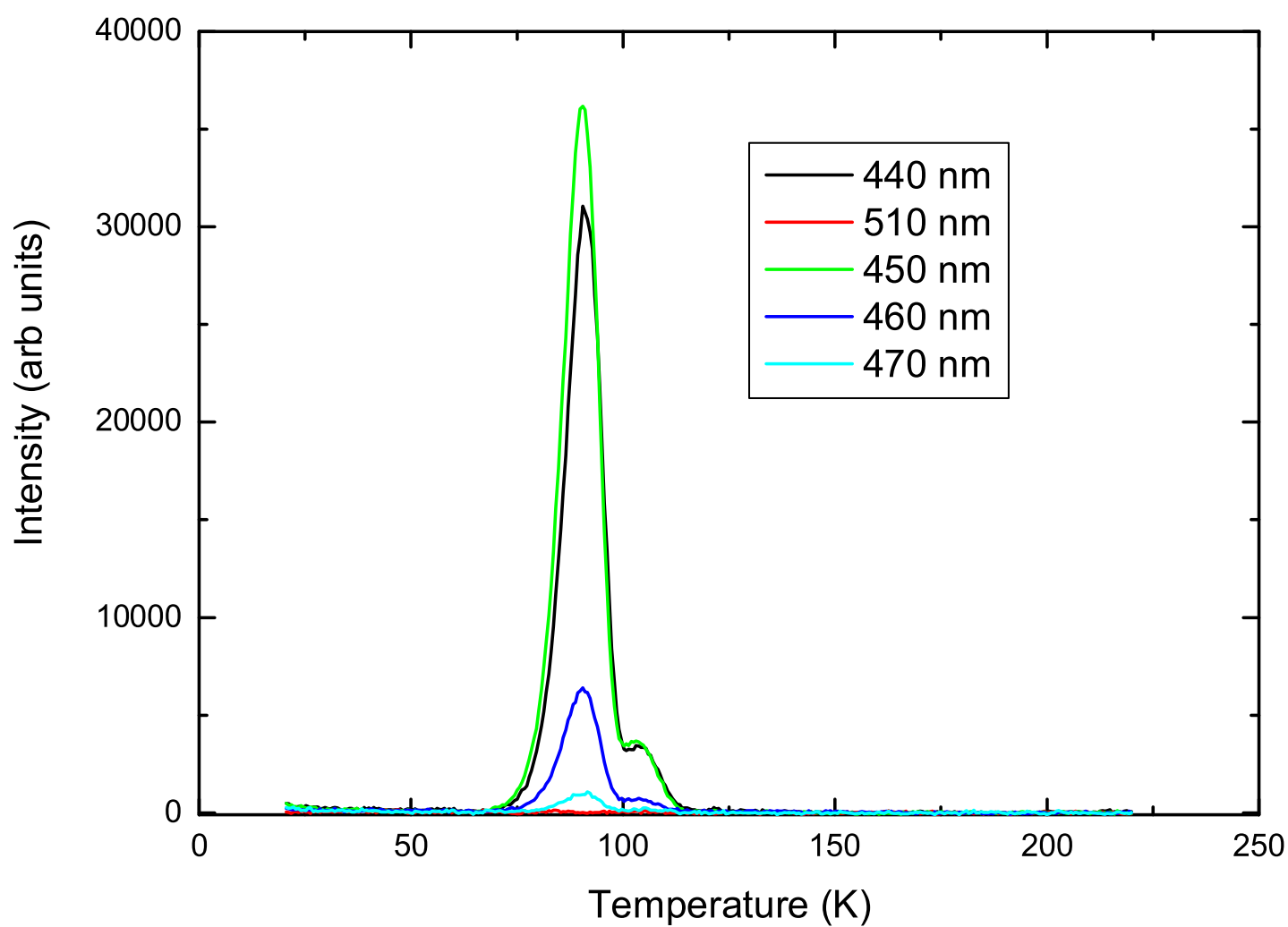


Figure 4.12: The glow curves for various excitation energies in Sr(SCN)<sub>2</sub>:Eu<sup>2+</sup>

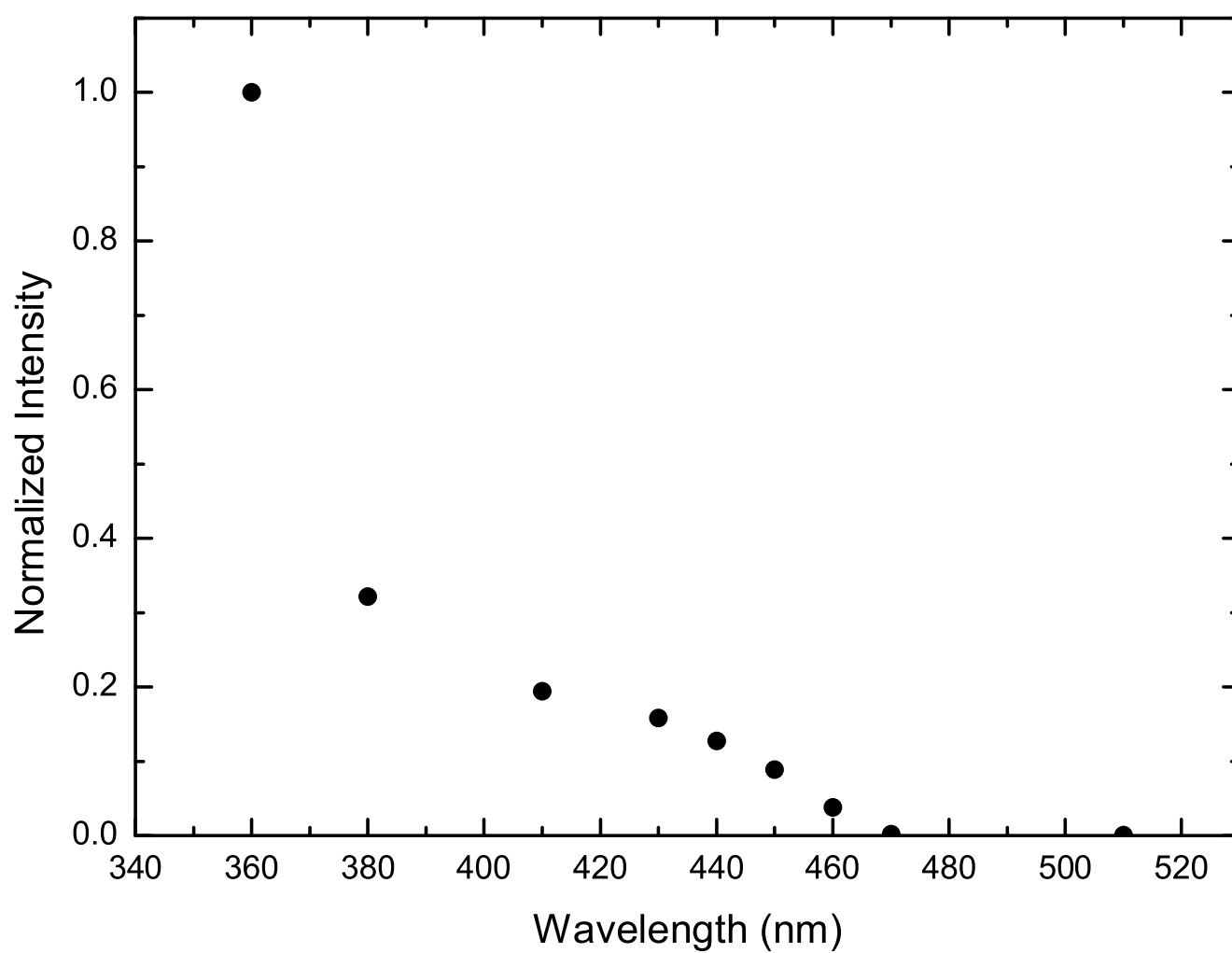


Figure 4.13: This graph shows the integrated glow curves plotted as a function of excitation wavelength, indicating a threshold at 450 nm.

analysis of the thermal quenching, we find the values to differ only by about  $680 \text{ cm}^{-1}$ :  $E_{PI}^{TSL} = 720 \text{ cm}^{-1}$ , and  $E_{PI}^{Arrh} = 1400 \text{ cm}^{-1}$ . Considering that the analysis of the thermal quenching was based on a very simplistic model, the small discrepancy of the results is astonishing.

## CHAPTER 5

### CONCLUSIONS

In this thesis we show that Thermally Stimulated Luminescence Excitation Spectroscopy has been applied successfully to measure the photoionization energy in a highly hygroscopic material. Comparing our results with those obtained from the analysis of thermal quenching, we find ionization energy values that differ by less than 0.1 eV. Further studies will focus on the refinement of the Arrhenius model and experimental investigation of the related system  $\text{Ba}(\text{SCN})_2:\text{Eu}^{2+}$ .

## 5.1 REFERENCES

- [1] G. F. Imbusch *Optical Spectroscopy of Inorganic Solids*
- [2] U. Happek, S. A. Basun, J. Choi, J. K. Krebs and M. Raukas *Electron transfer processes in rare earth doped insulators Journal of Alloys and Compounds, Volumes 303-304, 24 May 2000*
- [3] Jacques I. Pankove *Optical Processes in Semiconductors*
- [4] Charles Kittel *Introduction to Solid State Physics* 7<sup>th</sup> edition
- [5] Shigeo Shionoya, W. M. Yen, *Phosphor Handbook*
- [6] Michael D. Lumb, *Luminescence Spectroscopy*
- [7] S. W. S. McKeever, *Thermoluminescence of Solids*
- [8] *G. Blasse, B.C. Grabmaier*
- [9] J.T. Randall and M.H.F. Wilkins, *Proc. Roy. Soc. London* 184 (1945a) 366.
- [10] Claudia Wickleder *J of Alloys and Compounds*, 374(2004) 10-13
- [11] P. Dorenbos, *J. Lumin.* 104 (2003) 239.
- [12] J. Rubio, *J. Phys. Chem. Solids* 52 (1991) 101.
- [13] C. Wickleder *Chem. Mater.*, *in press*